Plant Cell Physiol. 48(12): 1659–1672 (2007)
doi:10.1093/pcp/pcm155, available FREE online at www.pcp.oxfordjournals.org

Rapid paper

The *PARVUS* Gene is Expressed in Cells Undergoing Secondary Wall Thickening and is Essential for Glucuronoxylan Biosynthesis

Chanhui Lee [1], Ruiqin Zhong [1], Elizabeth A. Richardson [1], David S. Himmelsbach [2], Brooks T. McPhail [2] and Zheng-Hua Ye [1,*]

[1] *Department of Plant Biology, University of Georgia, Athens, GA 30602, USA*
[2] *Richard B. Russell Agriculture Research Center, US Department of Agriculture, Agriculture Research Service, Athens, GA 30604, USA*

Xylan, cellulose and lignin are the three major components of secondary walls in wood, and elucidation of the biosynthetic pathway of xylan is of importance for potential modification of secondary wall composition to produce wood with improved properties. So far, three *Arabidopsis* glycosyltransferases, FRAGILE FIBER8, IRREGULAR XYLEM8 and IRREGULAR XYLEM9, have been implicated in glucuronoxylan (GX) biosynthesis. In this study, we demonstrate that PARVUS, which is a member of family GT8, is required for the biosynthesis of the tetrasaccharide primer sequence, β-D-Xyl-(1 → 3)-α-L-Rha-(1 → 2)-α-D-GalA-(1 → 4)-D-Xyl, located at the reducing end of GX. The *PARVUS* gene is expressed during secondary wall biosynthesis in fibers and vessels, and its encoded protein is predominantly localized in the endoplasmic reticulum. Mutation of the *PARVUS* gene leads to a drastic reduction in secondary wall thickening and GX content. Structural analysis of GX using ^{1}H-nuclear magnetic resonance (NMR) spectroscopy revealed that the *parvus* mutation causes a loss of the tetrasaccharide primer sequence at the reducing end of GX and an absence of glucuronic acid side chains in GX. Activity assay showed that the xylan xylosyltransferase and glucuronyltransferase activities were not affected in the *parvus* mutant. Together, these findings implicate a possible role for PARVUS in the initiation of biosynthesis of the GX tetrasaccharide primer sequence and provide novel insights into the mechanisms of GX biosynthesis.

Keywords: *Arabidopsis* — Glucuronoxylan biosynthesis — Glycosyltransferase — *PARVUS* — Secondary wall biosynthesis.

Abbreviations: CFP, cyan fluorescent protein; DTT, dithiothreitol; ER, endoplasmic reticulum; *fra8*, *fragile fiber8*; GalA, galacturonic acid; GlcA, glucuronic acid; GlcAT, glucuronyltransferase; GT, glycosyltransferase; GX, glucuronoxylan; *irx8*, irregular xylem*8*; irx*9*, *irregular xylem9*; MALDI-TOF MS, matrix-assisted laser-desorption ionization time-of-flight mass spectrometry; MeGlcA, 4-*O*-methyl-glucuronic acid; NMR, nuclear magnetic resonance; PBS, phosphate-buffered saline; YFP, yellow fluorescent protein; Xyl, xylose; XylT, xylosyltransferase.

Introduction

Cellulose, xylan and lignin are the three principal components of dicot wood. Because of the importance of wood in human life, it is imperative to elucidate the mechanisms involved in the biosynthesis and regulation of wood components. Knowledge gained from such studies will potentially allow us to modify cell wall composition on the basis of our needs, such as engineering walls more suitable for biofuel production. Although the biosynthetic genes for cellulose and lignin have been well characterized, our understanding of genes involved in xylan biosynthesis is limited.

Xylan is composed of a linear backbone of (1,4)-linked β-D-xylosyl (Xyl) residues with an average degree of polymerization from 90 to 120 (Johansson and Samuelson 1977, Pena et al. 2007). About 10% of Xyl residues on the backbone are substituted with α-D-glucuronic acid (GlcA), 4-*O*-methyl-α-D-glucuronic acid (MeGlcA) and/or α-D-arabinose at *O*-2 and/or *O*-3, and the Xyl residues may be acetylated on C-2 or C-3 (Ebringerová and Heinze 2000). Based on the nature of substitutions, xylan is typically named (methyl)glucuronoxylan (GX), which is the main hemicellulose in dicot wood, and arabinoxylan and glucuronoarabinoxylan, which are the most abundant hemicelluloses in grass cell walls (Ebringerová and Heinze 2000).

The biosynthesis of the xylan backbone and its side chains requires at least five types of enzymes, including xylosyltransferases (XylTs), glucuronyltransferases (GlcATs), arabinosyltransferases, methyltransferases and acetyltransferases. The activities of XylT, GlcAT, arabinosyltransferase and methyltransferases involved in xylan biosynthesis have been biochemically studied in a number of plant species (Dalessandro and Northcote 1981, Baydoun et al. 1983, Baydoun et al. 1989, Suzuki et al. 1991, Porchia and Scheller 2000, Kuroyama and Tsumuraya 2001, Gregory et al. 2002, Porchia et al. 2002, Urahara et al.

*Corresponding author: E-mail, zhye@plantbio.uga.edu; Fax, +1-706-542-1805.

2004). Recently, the *IRREGULAR XYLEM9* (*IRX9*) gene, which encodes a putative glycosyltransferase (GT) belonging to family GT43 (Coutinho et al. 2003), has been found to be essential for normal xylan backbone biosynthesis. The *IRX9* gene is expressed in cells undergoing the biosynthesis of secondary walls including GX, and its encoded protein is localized in the Golgi, where GX is synthesized (Pena et al. 2007). Mutation of the *IRX9* gene causes a reduction in the GX level (Brown et al. 2005, Bauer et al. 2006) as well as a substantial decrease in GX chain length (Pena et al. 2007). The defective GX chain elongation caused by the *irx9* mutation is correlated with a deficiency in xylan XylT activity (Lee et al. 2007). IRX9 is the first GT known to be required for normal xylan XylT activity. Both genetic and biochemical analyses suggest that IRX9 is a putative xylan synthase required for GX backbone elongation (Lee et al. 2007, Pena et al. 2007). The poplar GT43A/B, which is a homolog of IRX9 and expressed during wood formation (Aspeborg et al. 2005), is also probably responsible for GX backbone elongation in the secondary walls of wood because PoGT43B can functionally complement the GX and XylTase deficiency caused by the *irx9* mutation (Lee et al. 2007, Zhou et al. 2007).

In addition to the β-(1,4)-linked D-Xyl residues in the backbone, the reducing end of GX from birch, spruce and *Arabidopsis* has been found to contain a distinct tetrasaccharide primer sequence β-D-Xyl-(1 → 3)-α-L-Rha-(1 → 2)-α-D-GalA-(1 → 4)-D-Xyl (Shimizu et al. 1976, Johansson and Samuelson 1977, Anderson et al. 1983, Pena et al. 2007). Conceivably, at least four additional GTs are required for the biosynthesis of the tetrasaccharide primer sequence. So far, two GT genes, *FRAGILE FIBER8* (*FRA8*) and *IRX8*, which encode proteins belonging to GT families 47 and 8 (Coutinho et al. 2003), respectively, have been implicated in the biosynthesis of the tetrasaccharide primer sequence at the GX reducing end. Both *FRA8* and *IRX8* are specifically expressed in cells undergoing secondary wall biosynthesis, and their encoded proteins are localized in the Golgi (Zhong et al. 2005b, Pena et al. 2007). Mutations of the *FRA8* and *IRX8* genes result in a reduction in the level of GX (Brown et al. 2005, Zhong et al. 2005b, Pena et al. 2007, Persson et al. 2007) and a near absence of the tetrasaccharide primer sequence, indicating that FRA8 and IRX8 are involved in the biosynthesis of the tetrasaccharide primer sequence at the GX reducing end (Pena et al. 2007). Because family GT47 enzymes to which FRA8 belongs have inverting mechanisms and catalyze the formation of β-glycosidic linkages using α-linked nucleotide sugars or vice versa, FRA8 was proposed to catalyze the β-linkage of Xyl to *O*3 of rhamnose using UDP-α-D-Xyl as a substrate or the α-linkage of rhamnose to *O*2 of galacturonic acid (GalA) using UDP-β-L-rhamnose (Pena et al. 2007). Since family GT8 enzymes of which IRX8 is a member have retaining mechanisms and typically catalyze the formation of α-glycosidic linkages using α-linked nucleotide sugars, IRX8 was proposed to catalyze the α-linkage of GalA to *O*4 of the reducing Xyl residue of the tetrasaccharide primer sequence (Pena et al. 2007). The poplar GT47C, which is a homolog of FRA8 and expressed during wood formation, is also probably involved in the biosynthesis of the tetrasaccharide primer sequence at the reducing end of GX in secondary walls of wood (Zhou et al. 2006).

As described above, three GT genes have been implicated in various steps of GX biosynthesis. However, at least nine different enzymes are required for the biosynthesis of GX, arabinoxylan and glucuronoarabinoxylan. To further our understanding of the xylan biosynthetic pathway, it is necessary to identify and characterize additional xylan biosynthetic genes. In this study, we report that the *PARVUS* gene, which encodes a protein belonging to family GT8, is another GT required for GX biosynthesis. We show that the *PARVUS* gene is expressed during secondary wall biosynthesis and its encoded protein is localized in the endoplasmic reticulum (ER). We demonstrate that mutation of the *PARVUS* gene leads to a reduction in GX content and a loss of the tetrasaccharide primer sequence at the GX reducing end. Considering the fact that PARVUS is associated with the ER, it is tempting to propose that PARVUS is involved in the first transfer of the reducing Xyl residue of the tetrasaccharide primer sequence at the GX reducing end to an unknown acceptor at ER.

Results

Expression of the PARVUS gene is associated with secondary wall thickening

The interfascicular fibers of *Arabidopsis* inflorescence stems deposit a large amount of cellulose, xylan and lignin in secondary walls, which have been used as a model for studying genes involved in secondary wall biosynthesis (Zhong et al. 2001, Zhong et al. 2005b, Pena et al. 2007). To find genes responsible for xylan biosynthesis, we analyzed GTs that were up-regulated during secondary wall thickening using interfascicular fibers isolated by laser microdissection (Zhong et al. 2006). In this report, we studied the function of a putative GT gene, At1g19300, which was induced during secondary wall thickening of fibers. The At1g19300 gene is a member of GT family 8 (Coutinho et al. 2003) and was previously named *PARVUS*/*GLZ1*/*GATL1* (Lao et al. 2003, Shao et al. 2004, Sterling et al. 2006) and proposed to be involved in pectin biosynthesis (Lao et al. 2003, Lerouxel et al. 2006). We have found that

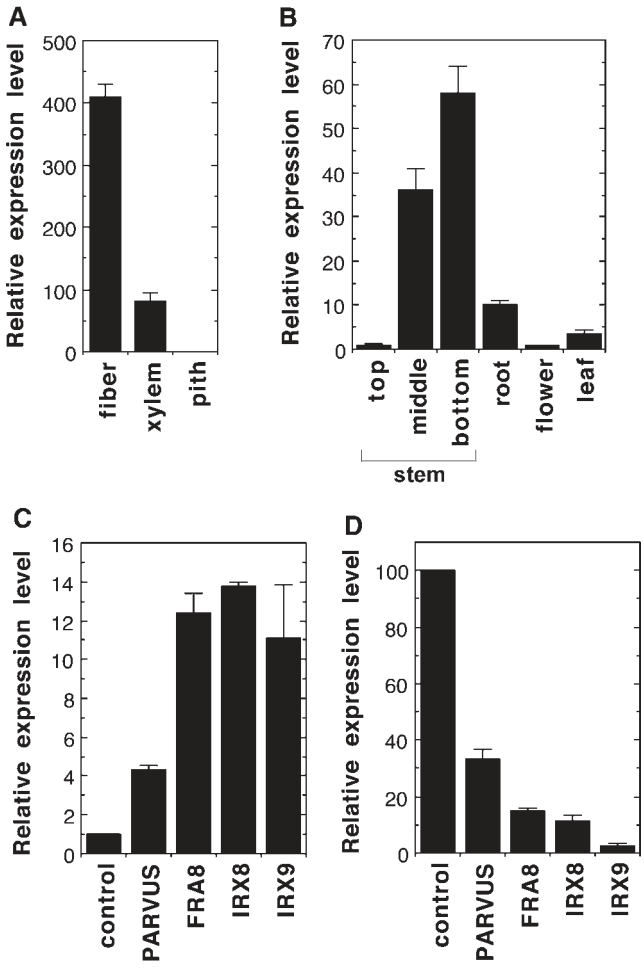

Fig. 1 Expression analysis of the *PARVUS* gene by real-time quantitative PCR. Error bars represent the SE of three replicates. (A) The *PARVUS* gene is highly expressed in interfascicular fibers and xylem cells, but absent in pith cells. The cells used for expression analysis were laser-microdissected from *Arabidopsis* stem sections. (B) The *PARVUS* gene exhibits predominant expression in stems undergoing secondary wall thickening. (C) The expression of *PARVUS* together with three other secondary wall biosynthetic genes, *FRA8*, *IRX8* and *IRX9*, is induced by MYB46 overexpression, which results in ectopic deposition of secondary walls. (D) The expression of *PARVUS*, *FRA8*, *IRX8* and *IRX9* is down-regulated in SND1/NST1 RNAi lines, which exhibit a loss of secondary wall thickening in fiber cells.

the *PARVUS* gene is highly expressed in fibers and xylem cells undergoing secondary wall thickening, but not in parenchymatous pith cells (Fig. 1A). At the organ level, the *PARVUS* gene is predominantly expressed in stems in which abundant secondary wall-containing fibers and xylem cells are produced (Fig. 1B). In addition, the expression of the *PARVUS* gene was shown to be co-induced with three known xylan biosynthetic genes, *FRA8*, *IRX8* and *IRX9*, by overexpression of MYB46 (Fig. 1C), which results in ectopic deposition of secondary walls (Zhong et al. 2007a). Moreover, its expression was down-regulated together with *FRA8*, *IRX8* and *IRX9* in SND1/NST1 RNA interference (RNAi) lines (Fig. 1D), which exhibit a loss of secondary wall thickening in fiber cells (Zhong et al. 2007b). Therefore, we reasoned that PARVUS is likely to be involved in the biosynthesis of a secondary wall component, such as GX, rather than pectin as previously proposed.

We next performed in situ mRNA localization to investigate the developmental expression pattern of the *PARVUS* gene in *Arabidopsis* stems and roots. In rapidly elongating internodes in which protoxylem is the only secondary wall-containing tissue present, the *PARVUS* mRNA signal was seen in the developing vessels of the protoxylem (Fig. 2A). At this stage, interfascicular fiber cells are undergoing rapid elongation and no secondary wall thickening is evident (Ye et al. 2002). Concomitantly, no *PARVUS* mRNA signal was seen in interfascicular fiber cells (Fig. 2A). In non-elongating internodes in which secondary wall thickening is evident in interfascicular fibers, a strong *PARVUS* mRNA signal was detected in interfascicular fiber cells in addition to developing vessels and xylary fibers in metaxylem (Fig. 2B). The *PARVUS* mRNA signal was also observed in developing vessels and xylary fibers in secondary xylem of roots (Fig. 2C). The control stem section hybridized with the sense *PARVUS* RNA probe did not show any positive signals (Fig. 2D). These results demonstrate that the *PARVUS* gene is specifically expressed in cells undergoing secondary wall thickening, including interfascicular fibers, vessels and xylary fibers. The secondary wall-associated expression pattern of the *PARVUS* gene revealed in this study differs from that reported in a previous study, which employed the promoter–β-glucuronidase (GUS) reporter gene analysis and showed its expression in almost all cell types in stems (Shao et al. 2004). It is apparent that the promoter used in the expression study lacks some regulatory elements required for the endogenous gene expression.

The PARVUS protein is associated with the ER

The PARVUS protein is predicted to have a hydrophobic signal peptide sequence at the N-terminus (Fig. 3A; Lao et al. 2003) by both protein hydropathy analysis and the prediction of protein sorting signals and localization sites program (PSORT; http://psort.ims.u-tokyo.ac.jp/). To examine the subcellular localization of the PARVUS protein, we co-expressed yellow fluorescent protein (YFP)-tagged PARVUS with a cyan fluorescent protein (CFP)-tagged ER marker and a Golgi marker in carrot (*Daucus carota*) protoplasts, and studied their co-localization patterns. It was found that the fluorescent signals of PARVUS–YFP displayed a network-like pattern, which clearly overlapped with the localization pattern of the

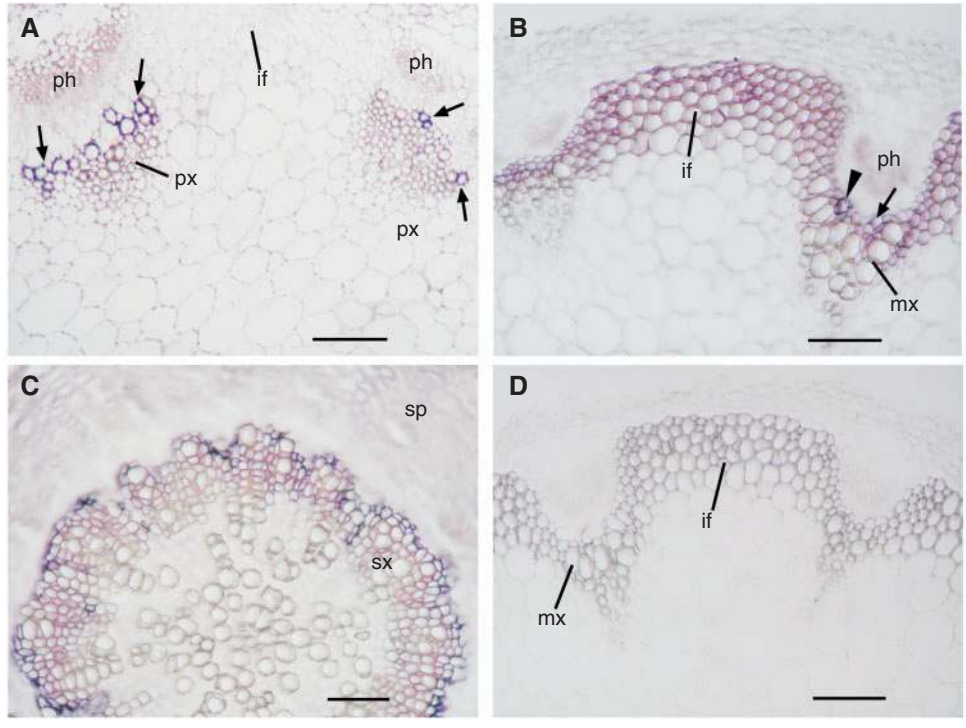

Fig. 2 In situ hybridization analysis of the *PARVUS* mRNA in *Arabidopsis* stems and roots. Cross-sections of stems and roots of wild-type plants were hybridized with digoxigenin-labeled *PARVUS* antisense (A–C) or sense (D) RNA probe, and subsequently detected with alkaline phosphate-conjugated antibodies. The hybridization signals are shown as purple color. (A) Cross-section of the elongating part of a stem showing the predominant expression of *PARVUS* in developing vessels (arrows). (B) Cross-section of the non-elongating part of a stem showing the expression of *PARVUS* in interfascicular fibers, xylary fibers (arrow) and developing vessels (arrowheads), all of which are undergoing extensive secondary wall thickening. (C) Cross-section of a root showing the predominant expression of *PARVUS* in the developing secondary xylem. (D) A control section of the non-elongating part of a stem hybridized with the sense *PARVUS* probe showing the absence of hybridization signals. if, interfascicular fiber; mx, metaxylem; px, protoxylem; sx secondary xylem. Bars = 204 μm.

ER marker (Fig. 3D–G). In contrast, the network-like signals of PARVUS–YFP displayed apparent differences from the punctate localization pattern of FRA8–CFP (Fig. 3H–K) that is known to be localized in the Golgi (Zhong et al. 2005a), although some overlap of signals was observed. The control protoplasts expressing YFP alone had fluorescent signals distributed throughout the cytoplasm (Fig. 3B, C). These results indicate that the PARVUS protein is predominantly associated with the ER.

Mutation of the PARVUS gene causes a severe reduction in secondary wall thickening of fibers and vessels

The finding that the *PARVUS* gene is specifically expressed in cells undergoing secondary wall thickening suggests that it is likely to be involved in secondary wall biosynthesis. To find out whether the *PARVUS* gene is essential for secondary wall thickening, we obtained a homozygous T-DNA insertion knockout line of *PARVUS* (SALK_045368; obtained from ABRC, Columbus, OH, USA) for examination of stem strength and wall thickness of fibers and vessels. The homozygous T-DNA knockout plants were smaller in rosette size and their stems exhibited a dwarf phenotype, which is identical to the previously reported observations for *parvus* mutations (Lao et al. 2003, Shao et al. 2004). It was found that mutation of the *PARVUS* gene led to a severe reduction in the mechanical strength of stems compared with the wild type (Fig. 4A). Examination of fibers and vessels in stems and roots revealed that the wall thickness of fibers and vessels in the *parvus* mutant was drastically decreased compared with the wild type (Fig. 4B–G). It was apparent that the vessels in the *parvus* mutant exhibited a collapsed phenotype, which is most probably caused by the reduced wall strength as observed in other known secondary wall-defective mutants (Brown et al. 2005, Zhong et al. 2005b, Persson et al. 2005). Transmission electron microscopy showed that the wall thickness of interfascicular fibers, vessels and xylary fibers was reduced by 50–66% compared with the wild type (Fig. 5; Table 1). These results suggest that PARVUS is required for normal secondary wall thickening in both fibers and vessels.

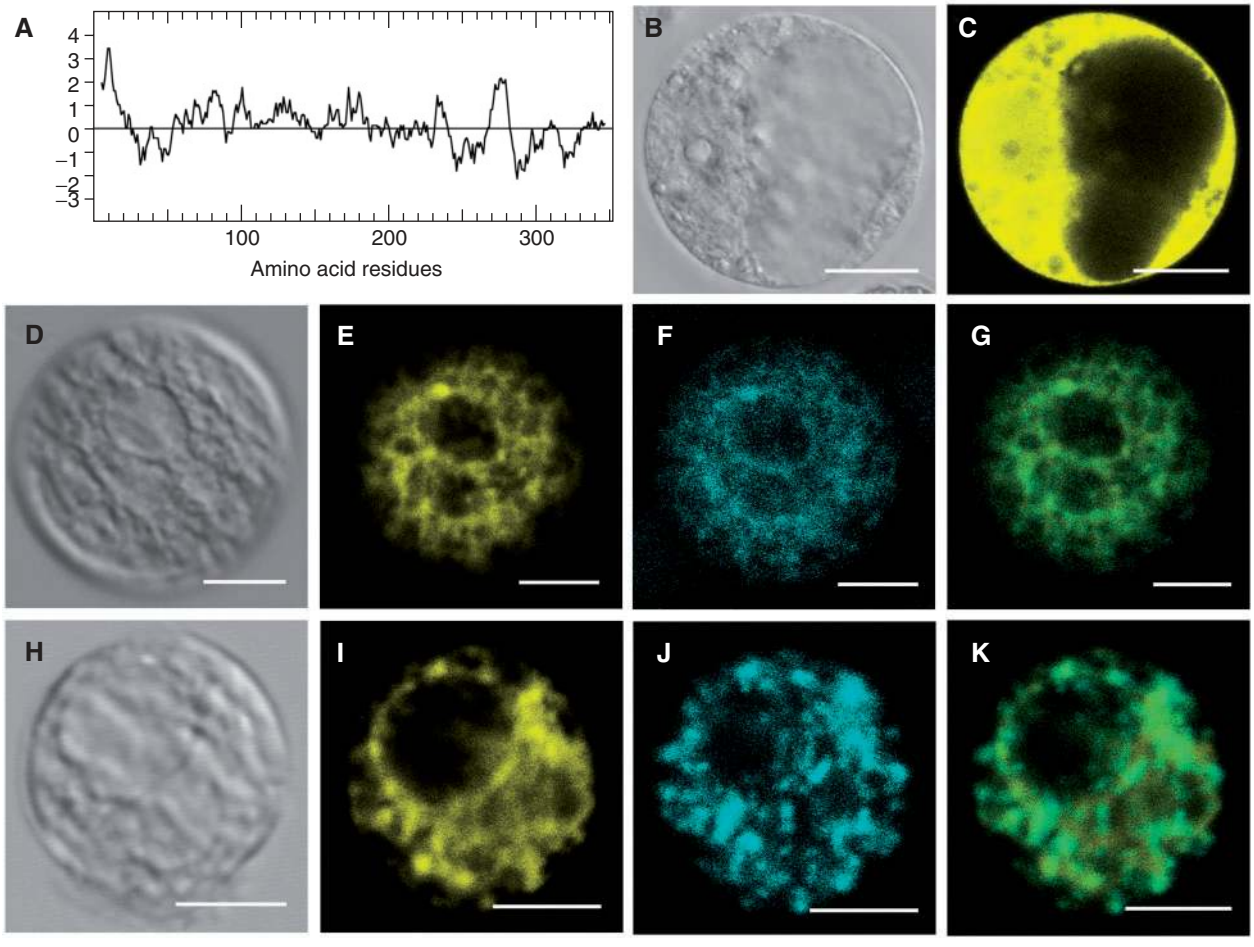

Fig. 3 Subcellular localization of the PARVUS protein. Yellow fluorescent protein (YFP)-tagged PARVUS together with cyan fluorescent protein (CFP)-tagged subcellular organelle markers were co-expressed in carrot protoplasts, and their fluorescent signals were visualized with a laser confocal microscope. (A) Hydropathy plot of the PARVUS protein showing the presence of a signal peptide sequence at the N terminus. (B) and (C) Differential interference contrast (DIC) image (B) and the corresponding fluorescent signals (C) of a carrot protoplast expressing YFP alone. (D–G) DIC image (D) and the corresponding PARVUS–YFP signals (E), ER–CFP signals (F) and the merged image (G) of a carrot cell expressing PARVUS–YFP and the ER marker ER–CFP. Note the close superimposition of PARVUS–YFP and ER–CFP signals. (H–K) DIC image (H) and the corresponding PARVUS–YFP signals (I), FRA8–CFP signals (J) and the merged image (K) of a carrot cell expressing PARVUS–YFP and the Golgi-localized FRA8–CFP. Note the differences between the network localization pattern of PARVUS–YFP and the punctate pattern of FRA8–CFP. Bars = 35 μm.

Mutation of the PARVUS gene results in a reduction in GX content in stems and a loss of LM10 antibody labeling of xylan in secondary walls of fibers and vessels

The observation that PARVUS is associated with the ER indicates that it is involved in the biosynthesis of a non-cellulosic polysaccharide. Because the major non-cellulosic polysaccharide in secondary walls of *Arabidopsis* fibers and vessels is GX, we postulate that PARVUS might play a role in GX biosynthesis. To investigate which secondary wall components are affected by the *parvus* mutation, we first analyzed the composition of total cell walls isolated from stems and found that the amount of xylose and glucose, which are the respective main components of GX and cellulose, was reduced by 46.7 and 23.5%, respectively, compared with the wild type (Table 2). No significant alterations were seen in the amount of other cell wall neutral sugars, including mannose, galactose, arabinose, rhamnose and fucose. Further composition analysis of 1 and 4 N KOH extracts of cell walls from stems of wild type and *parvus* showed that the most drastically reduced sugar content was xylose (Table 3). Because the xylose in 1 and 4 N KOH extracts of *Arabidopsis* stems comes primarily from GX (Zhong et al. 2005b), these findings strongly suggest that PARVUS is involved in GX biosynthesis. The reduction in cellulose content in the *parvus* mutant is probably due to an indirect effect, which has also been

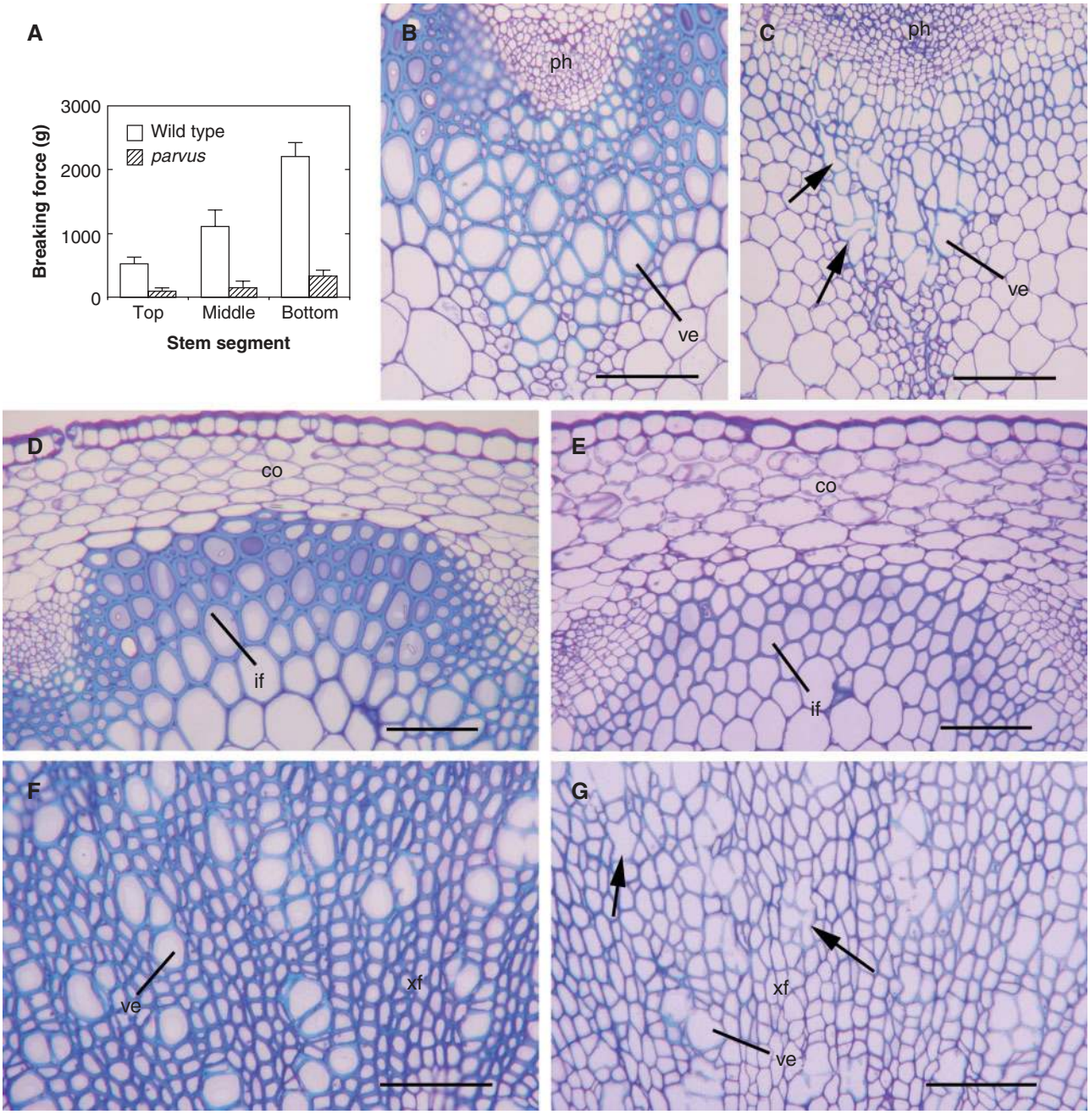

Fig. 4 Mutation of the *PARVUS* gene results in a dramatic reduction in stem strength and wall thickness of fibers and vessels. Inflorescence stems of 10-week-old plants were used for breaking strength measurement, and the bottom internodes and roots were sectioned for examination of fibers and vessels. (A) Breaking force measurement showing a drastic reduction in stem strength in the *parvus* mutant compared with the wild type. Error bars represent the SE of measurements of 20 plants. (B) and (C) Cross-sections of stems showing vascular bundles of the wild type (B) and *parvus* mutant (C). Note that the vessels in the *parvus* mutant are severely deformed (arrows). (D) and (E) Cross-sections of interfascicular regions of stems showing the drastically reduced fiber wall thickness in *parvus* (E) compared with the wild type (D). (F) and (G) Cross-sections of roots showing the thin walled vessels and fibers in secondary xylem in the *parvus* mutant (F) compared with the wild type (G). Note the severely deformed vessels in the *parvus* mutant (arrows). co, cortex; if, interfascicular fiber; ph, phloem; ve, vessel; xf, xylary fiber. Bars = 141 μm.

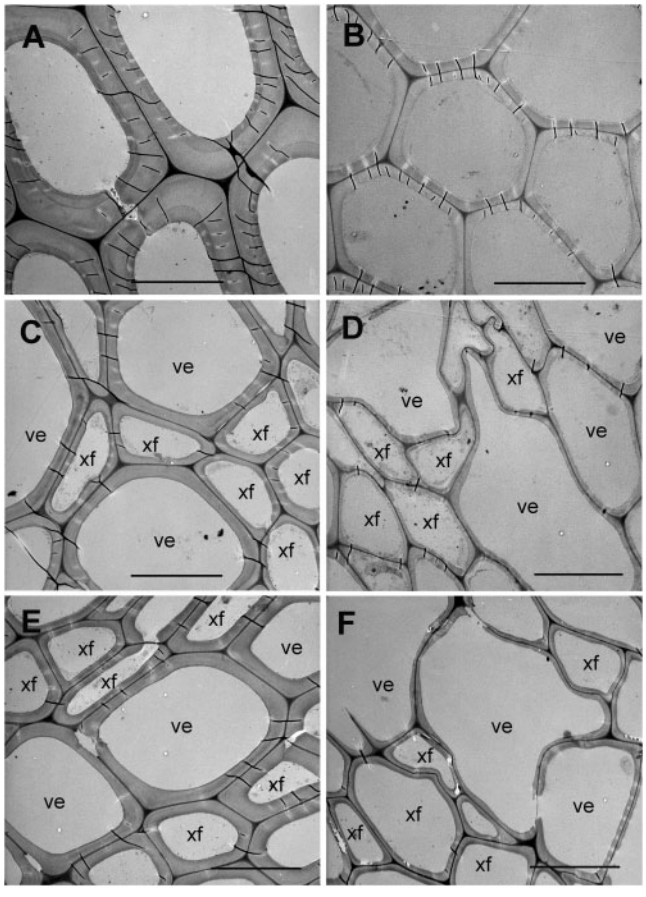

Fig. 5 Transmission electron microscopy of secondary walls of fibers and vessels in the *parvus* mutant. (A) and (B) Interfascicular fiber cells of stems showing their thin walls in *parvus* (B) compared with the wild type (A). (C) and (D) Vessels and xylary fibers of stems showing their thin walls in *parvus* (D) compared with the wild type (C). Note the deformation of vessels. (E) and (F) Vessels and xylary fibers in root secondary xylem showing their thin walls in *parvus* (F) compared with the wild type (E). Note the deformation of vessels. ve, vessel; xf, xylary fiber. Bars = 7.9 μm.

observed in three other known xylan-deficient mutants (Brown et al. 2005, Zhong et al. 2005b). The *parvus* mutation has previously been shown to reduce the xylose content in leaf cell walls, which was attributed to an indirect effect due to its presumed role in pectin biosynthesis (Lao et al. 2003). Because PARVUS is a GT believed to be involved in polysaccharide synthesis but is unlikely to be involved in lignin synthesis, we did not analyze the possible effect of its mutation on lignin alterations.

To substantiate the role of PARVUS in GX biosynthesis, we next examined the effect of the *parvus* mutation on GX deposition by immunolocalization using monoclonal antibody LM10 that binds to 4-*O*-methylglucuronoxylan (McCartney et al. 2005). Immunolabeling of wild-type stem and root sections showed intensive fluorescent signals in the walls of interfascicular fibers and xylem cells including vessels and xylary fibers (Fig. 6A, D), all of which are known to contain abundant GX in secondary walls. In contrast, almost no fluorescent signals were observed in the secondary wall-containing tissues in *parvus* stems and roots (Fig. 6B, E). Expression of the wild-type *PARVUS* gene in the *parvus* mutant restored the xylan signals to the wild-type level in all secondary wall-containing tissues in stems and roots (Fig. 6C, F). These results demonstrate that PARVUS is required for the normal biosynthesis and deposition of GX in secondary walls of fibers and vessels.

The parvus mutation leads to an absence of non-methylated GlcA side chains in GX

To determine whether mutation of the *PARVUS* gene affects the GX structure, the KOH-solubilized GX from stems of wild type and the *parvus* mutant was digested with endoxylanase, and the acidic xylooligosaccharides produced by the digestion were analyzed by matrix-assisted laser-desorption ionization time-of-flight mass spectrometry (MALDI-TOF MS). MALDI-TOF MS of the wild-type acidic xylooligosacchrides revealed two major ion peaks $[M + Na]^+$ at mass-to-charge ratios (m/z) of 743 and 759 (Fig. 7A), which are attributed to xylooligosaccharides with four Xyl residues substituted with one non-methylated α-D-GlcA or one 4-*O*-Me-α-D-GlcA, respectively (Fig. 7C; Zhong et al. 2005b). The xylooligosaccharides bearing 4-*O*-Me-α-D-GlcA side chains are more abundant than those bearing α-D-GlcA side chains, which is a typical pattern observed in the GX of wild-type *Arabidopsis* (Zhong et al. 2005b). In contrast, the MALDI-TOF spectrum of *parvus* acidic xylooligosacchrides contains only the ion peak at an m/z of 759 (Fig. 7B). The *parvus* mutant lacked the ion with an m/z of 743 that is attributed to xylotetrasaccharides substituted with one non-methylated α-D-GlcA. The MALDI-TOF analysis demonstrates that the *parvus* mutation results in a loss of α-D-GlcA side chains in GX.

The parvus mutation causes a loss of the tetrasaccharide primer sequence located at the reducing end of GX

The *Arabidopsis* GX contains a tetrasaccharide primer sequence located at the reducing end, which differs from the GX backbone (Pena et al. 2007). A previous study showed that FRA8 and IRX8 are required for the biosynthesis of this tetrasaccharide primer sequence (Pena et al. 2007). To investigate further the roles of PARVUS in GX biosynthesis, we examined whether the *parvus* mutation affects the biosynthesis of the tetrasaccharide primer sequence using nuclear magnetic resonance (NMR) spectrometry. The ^{1}H-NMR spectrum of wild-type acidic xylooligosaccharides contained anomeric resonances of H1 and H5 of α-D-GlcA and H1 of branched β-D-Xyl residues bearing an α-D-GlcA residue, as well as H1 and H5 of 4-*O*-Me-α-D-GlcA residues

Table 1 Wall thickness of fibers and vessels in the stems and roots of wild-type and *parvus* mutant plants

Sample	Interfascicular fibers	Stem		Root	
		Vessels	Xylary fibers	Vessels	Xylary fibers
Wild type	2.10 ± 0.36	1.01 ± 0.09	0.71 ± 0.18	1.16 ± 0.14	0.78 ± 0.21
Parvus	0.71 ± 0.21	0.45 ± 0.15	0.36 ± 0.07	0.54 ± 0.18	0.27 ± 0.10

Wall thickness was measured from transmission electron micrographs of fibers and vessels. Data are means (μm) ± SE from 20 cells.

Table 2 Monosaccharide composition of cell walls from the stems of wild-type and *parvus* plants

Sample	Glucose	Xylose	Mannose	Galactose	Arabinose	Rhamnose	Fucose
Wild type	306 ± 26	122 ± 4	20.7 ± 0.6	14.9 ± 2.4	13.7 ± 1.7	8.0 ± 1.0	2.5 ± 0.6
Parvus	234 ± 22	65 ± 5	25.2 ± 0.5	18.3 ± 0.7	17.4 ± 1.7	5.0 ± 0.6	1.6 ± 0.3

Cell wall residues used for composition analysis were prepared from stems of 10-week-old plants. Data are means (mg g^{-1} dry cell wall) ± SE of three independent assays.

Table 3 Monosaccharide composition of 1 and 4 N KOH extracts from the cell walls of wild-type and *parvus* plants

Cell wall sample	Xylose	Mannose	Galactose	Arabinose	Rhamnose	Fucose	Glucose
1 N KOH extract							
Wild type	44.5 ± 10.5	0.7 ± 0.1	3.5 ± 0.4	3.2 ± 0.7	2.7 ± 0.7	0.6 ± 0.1	11.4 ± 0.6
Parvus	9.9 ± 0.5	1.4 ± 0.1	4.9 ± 0.4	4.5 ± 0.4	2.8 ± 0.2	0.5 ± 0.2	6.9 ± 0.1
4 N KOH extract							
Wild type	30.2 ± 4.0	8.6 ± 0.5	6.6 ± 0.7	2.8 ± 0.3	2.3 ± 0.2	2.1 ± 0.2	16.2 ± 1.0
Parvus	13.2 ± 1.6	7.8 ± 1.1	4.8 ± 0.6	2.2 ± 0.2	1.4 ± 0.1	1.4 ± 0.1	12.2 ± 1.5

Cell walls were extracted sequentially with 1 and 4 N KOH, and the alkali-soluble extracts were used for monosaccharide composition analysis. Data are means (mg g^{-1} dry cell wall) ± SE of two independent assays.

and H1 of branched β-D-Xyl residues bearing a 4-*O*-Me-α-D-GlcA residue (Fig. 8A). The spectrum also includes resonances of H1 of α-Xyl and β-Xyl residues at the reducing ends of oligoxylosaccharides and H1 of unbranched β-Xyl residues (Fig. 8A). Furthermore, the resonances assigned to the tetrasaccharide primer sequence β-D-Xyl-(1 → 3)-α-L-Rha-(1 → 2)-α-D-GalA-(1 → 4)-D-Xyl that is located at the reducing end of GX was apparent in the spectrum of wild-type acidic xylooligosaccharides (Fig. 8A). These resonances include H1 of α-D-GalA, H1 of α-L-Rha, H1 of 3-linked β-D-Xyl, H4 of α-D-GalA and H2 of α-L-Rha. The observed ^{1}H-NMR spectrum of wild-type acidic xylooligosaccharides is the same as that previously reported for wild-type *Arabidopsis* acidic xylooligosaccharides (Zhong et al. 2005, Pena et al. 2007). Examination of the ^{1}H-NMR spectrum of *parvus* acidic xylooligosaccharides showed an apparent lack of resonances of H1 of α-D-GalA, H1 of α-L-Rha, H1 of 3-linked β-D-Xyl, H4 of α-D-GalA, and H2 of α-L-Rha, which are assigned to the tetrasaccharide primer sequence β-D-Xyl-(1 → 3)-α-L-Rha-(1 → 2)-α-D-GalA-(1 → 4)-D-Xyl that is located at the reducing end of GX (Fig. 8B). In addition, the resonances assigned to H1 and H5 of α-D-GlcA and H1 of branched β-D-Xyl residues bearing an α-D-GlcA residue were absent in *parvus* (Fig. 8B), which is consistent with the MALDI-TOF data (Fig. 7). These results demonstrate that the *parvus* mutation leads to a loss of the tetrasaccharide primer sequence at the GX reducing end, which suggests that PARVUS is involved in the biosynthesis of the tetrasaccharide primer sequence.

The xylan xylosyltransferase and glucuronyltransferase activities are not affected by parvus mutation

To investigate whether the reduced GX content and altered GX structure were caused by a reduction in XylT or GlcAT activities, we performed comparative analysis of their activities using microsomes isolated from wild-type and *parvus* stems. It was found that there was no decrease in the XylT and GlcAT activities in the *parvus* mutant; instead they were elevated compared with the wild type (Fig. 9). The elevation of

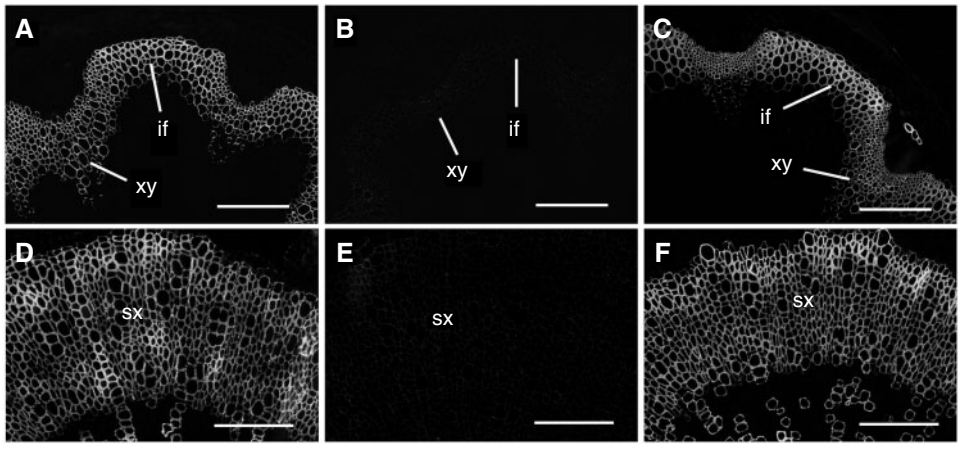

Fig. 6 Immunodetection of xylan in fibers and vessels of *parvus* stems and roots. Stem and root sections were probed with the monoclonal antibody LM10 that was generated against plant cell wall (1,4)-β-D-xylan. Xylan signals were detected with fluorescein isothiocyanate-conjugated secondary antibodies and visualized with a laser confocal microscope. (A–C) Xylan immunofluorescent signals in stem sections of the wild type (A), *parvus* mutant (B) and *parvus* complemented with the wild-type *PARVUS* gene (C). Note the absence of xylan signals in the walls of interfascicular fibers and xylem in the *parvus* mutant compared with the wild type. (D–F) Xylan immunofluorescent signals in root sections of the wild type (D), *parvus* mutant (E) and *parvus* complemented with the wild-type *PARVUS* gene (F). Note the absence of xylan signals in the walls of secondary xylem in the *parvus* mutant. if, interfascicular fiber, sx, secondary xylem; xy, xylem. Bars = 159 μm.

XylT and GlcAT activities was also observed in three other xylan-deficient mutants, *fra8*, *irx8* and *irx9* (Lee et al. 2007), probably due to a compensatory effect caused by these mutations. These results suggest that PARVUS is not required for the normal activities of xylan XylT and GlcAT.

Discussion

Xylan is the second most abundant polysaccharide in dicot wood, and thus understanding its biosynthetic pathway is of importance for rationally modifying secondary wall composition to produce wood with improved properties. At least nine different enzymes are needed in the multiple steps of xylan biosynthesis, including the initiation and elongation of xylan backbone, and addition and modification of xylan side chains. So far, one GT, IRX9, has been demonstrated to be required for normal xylan XylT activity and normal elongation of the xylan chain, and two other GTs, FRA8 and IRX8, have been shown to be required for the biosynthesis of the tetrasaccharide primer sequence at the reducing end of GX. Our identification of PARVUS as another GT essential for the biosynthesis of the tetrasaccharide primer sequence at the reducing end of GX marks another important step toward the elucidation of the complex process of xylan biosynthesis.

PARVUS is expressed during secondary wall biosynthesis and its encoded protein is associated with the ER

Gene expression analyses revealed that the *PARVUS* gene is expressed predominantly in cells undergoing secondary wall thickening (Figs. 1, 2), a pattern similar to that of three other known xylan biosynthetic genes (Zhong et al. 2005b, Pena et al. 2007, Persson et al. 2007). The secondary wall-associated expression pattern indicates that PARVUS is unlikely to be involved in the biosynthesis of a primary wall component, such as pectin, because there is little pectin present in secondary walls (Willats et al. 2001). The previous notion that PARVUS might be involved in pectin biosynthesis was primarily based on its sequence homology to other members of family GT8, QUASIMODO1 (Bouton et al. 2001) and GAUT1 (Sterling et al. 2006), and no genetic or biochemical data are available to substantiate such a proposed function. As discussed below, the secondary wall-associated expression pattern of PARVUS is consistent with its essential role in the biosynthesis of GX in secondary walls. The poplar GT8E/F, which is a close homolog of PARVUS, has also been shown to be expressed during wood formation (Aspeborg et al. 2005).

PARVUS was found to be predominantly localized in the ER, a localization pattern different from that of other known xylan biosynthetic enzymes, FRA8, IRX8 and IRX9, which are located in the Golgi (Zhong et al. 2005b, Pena et al. 2007). This difference is consistent with the sequence analysis showing that whereas FRA8, IRX8 and IRX9 are type II membrane proteins, PARVUS is predicted to contain a hydrophobic signal peptide sequence but no transmembrane helices. The ER localization of PARVUS suggests that it catalyzes a step that is different from FRA8, IRX8 and IRX9 in GX biosynthesis.

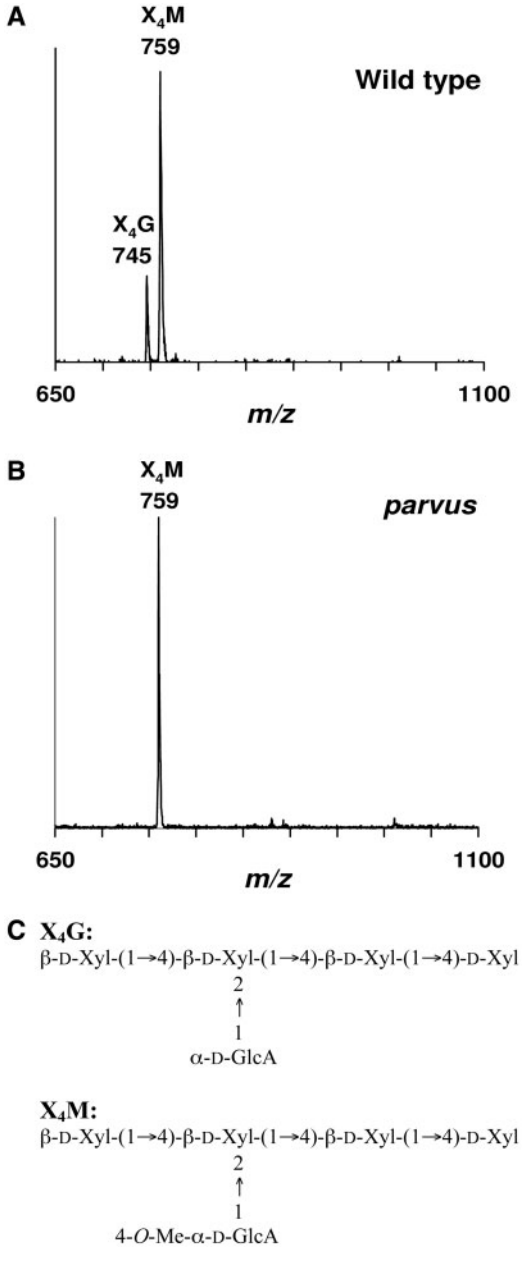

Fig. 7 MALDI-TOF mass spectra of acidic xylooligosaccharides generated by β-endoxylanase digestion of GX from the stems of the wild type (A) and *parvus* mutant (B). The ions at *m/z* 745 and 759 correspond to xylooligosaccharides composed of four Xyl residues bearing a non-methylated GlcA residue (X_4G) and a methylated GlcA residue (X_4M), respectively (C). Note the absence of the ion at *m/z* 745 corresponding to X_4G in the *parvus* mutant.

PARVUS is probably involved in the initiation of the biosynthesis of the GX tetrasaccharide primer sequence at the ER

Structural analysis of GX from the *parvus* mutant clearly demonstrates that PARVUS is involved in the biosynthesis of the tetrasaccharide primer sequence at the reducing end of GX. Thus, PARVUS joins FRA8 and IRX8 in the list of GTs required for the synthesis of the tetrasaccharide sequence. Based on their catalytic mechanisms, FRA8 has previously been proposed to catalyze the transfer of Xyl to rhamnose or rhamnose to GalA, whereas IRX8 was proposed to transfer GalA to the reducing Xyl residue at the GX reducing end (Pena et al. 2007). Because PARVUS belongs to family GT8 in which known members have retaining catalytic mechanisms and it is phylogenetically related to IRX8, it is possible that PARVUS and IRX8 function redundantly in catalyzing the addition of α-D-GalA to *O*4 of the reducing Xyl residue at the GX reducing end using UDP-α-D-GalA as a sugar donor. However, the fact that PARVUS is predominantly localized in the ER and IRX8 in the Golgi suggests that PARVUS catalyzes an enzymatic step earlier than IRX8 in the GX biosynthetic pathway.

One appealing hypothesis is that PARVUS is involved in the initiation of tetrasaccharide primer biosynthesis by catalyzing the transfer of the reducing Xyl residue onto an unknown acceptor in the ER. This scenario bears analogy to the biosynthesis of animal glycosaminoglycans. It has been shown that the biosynthesis of animal glycosaminoglycans requires a tetrasaccharide primer sequence, and the synthesis of the primer is initiated in the ER by transferring the reducing Xyl residue to protein and the subsequent steps of the tetrasaccharide primer synthesis occur in the Golgi (Prydz and Dalen 2000). A previous study has shown that GX is covalently attached to protein (Crosthwaite et al. 1994). Thus, it is possible that the GX tetrasaccharide primer synthesis is initiated in the ER where PARVUS might catalyze the transfer of the reducing Xyl residue to protein, which is then transported to the Golgi where subsequent additions of sugar residues are catalyzed by IRX8, FRA8 and other uncharacterized GTs.

It was previously proposed that the tetrasaccharide sequence at the reducing end of GX might function as a primer or as a chain terminator for GX biosynthesis (Pena et al. 2007). Our finding that PARVUS is predominantly localized in the ER and required for the synthesis of the tetrasaccharide sequence at the reducing end of GX favors the tetrasaccharide sequence as a primer for GX biosynthesis.

PARVUS is essential for the biosynthesis of a normal amount of GX and GlcA side chains

In addition to a loss of the tetrasaccharide sequence at the reducing end of GX, the *parvus* mutation also leads to a reduction in GX content and a loss of GlcA side chains. These phenotypes, which are also observed in three other xylan mutants, *fra8*, *irx8* and *irx9* (Brown et al. 2005, Zhong et al. 2005b, Bauer et al. 2006, Pena et al. 2007,

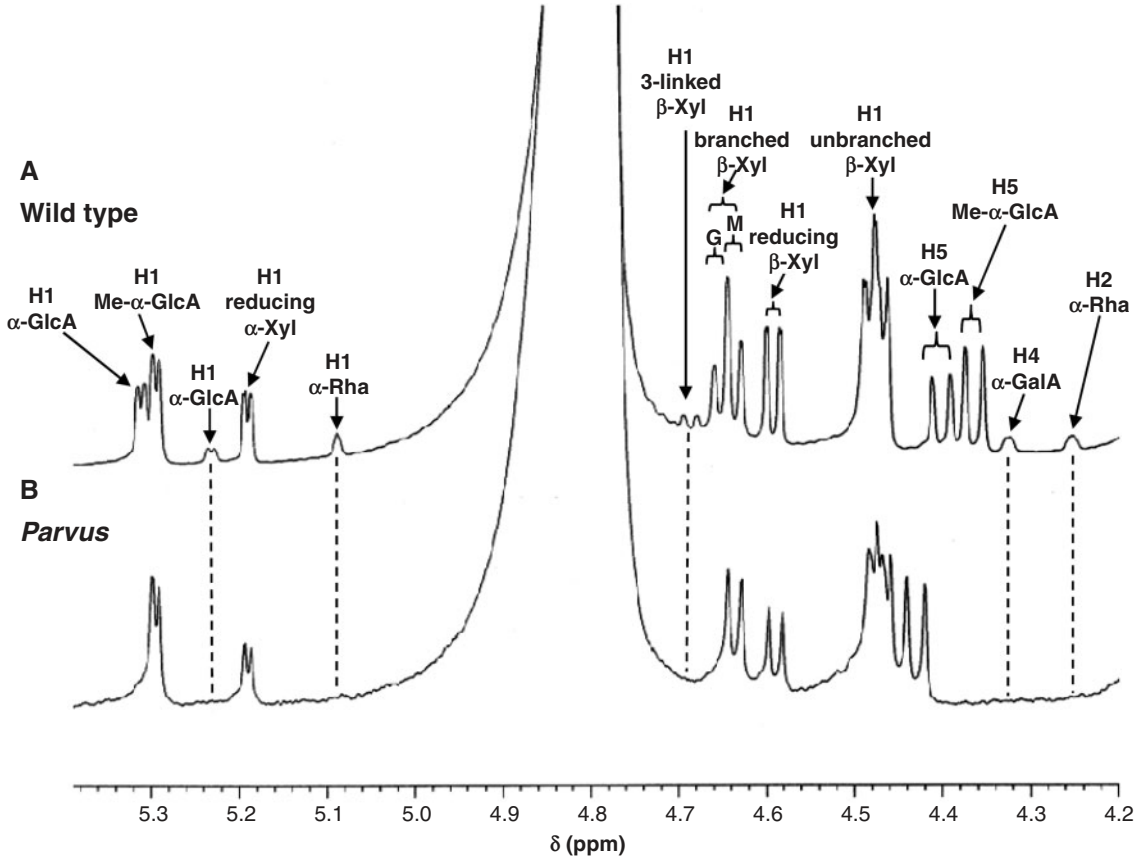

Fig. 8 Anomeric region of the ^{1}H-NMR spectra of xylooligosaccharides generated by β-endoxylanase digestion of GX from wild-type (A) and *parvus* (B) stems. Resonances are labeled with the position of the assigned proton and the identity of the residue containing that proton. G denotes the resonance of H1 of branched β-Xyl residues bearing an α-GlcA side chain. M denotes the resonance of H1 of branched β-Xyl residues bearing a 4-*O*-Me-α-GlcA side chain. The resonances of H5 of 4-*O*-Me-α-GlcA in *parvus* are shifted relative to those of the wild type. It is apparent that compared with the wild type, the *parvus* mutant lacks the resonances of H1 of α-D-GalA, H1 of α-L-Rha, H1 of 3-linked β-D-Xyl, H4 of α-D-GalA and H2 of α-L-Rha from the tetrasaccharide primer sequence located at the reducing end of GX as well as the resonances of H1 and H5 of α-GlcA residues, and H1 of branched β-Xyl residues bearing an α-GlcA residue.

Persson et al. 2007), are probably an indirect effect caused by the defects in the biosynthesis of the tetrasaccharide primer sequence. As proposed above, the tetrasaccharide sequence most probably functions as a primer for xylan backbone elongation, and thus a disruption in the biosynthesis of the primer sequence by the *parvus* mutation leads to an inhibition of GX biosynthesis. The loss of GlcA but not methylated GlcA side chains in GX could be explained by the saturation mechanism (Zhong et al. 2005, Pena et al. 2007). Because GlcA is methylated after it is transferred onto the GX backbone (Baydoun et al. 1989), it is possible that in the wild type, the methyltransferase activity could not keep up with the rate of GlcA addition and thus a proportion of GlcA side chains are not methylated. In contrast, the GX biosynthesis rate is greatly reduced in the *parvus* mutant, and thus the available methyltransferase activity could sufficiently methylate all GlcA side chains. This is consistent with the activity data showing that the *parvus* mutation does not affect the GlcAT activity (Fig. 9).

In summary, our study reveals an essential role for PARVUS in GX biosynthesis in secondary walls. We have demonstrated that PARVUS is required for the biosynthesis of the tetrasaccharide primer sequence, β-D-Xyl-(1 → 3)-α-L-Rha-(1 → 2)-α-D-GalA-(1 → 4)-D-Xyl, located at the reducing end of GX. Based on our findings, we propose that PARVUS is involved in the initiation of the biosynthesis of the tetrasaccharide sequence, which functions as a primer for subsequent GX biosynthesis. Our work provides foundation knowledge for further dissecting the mechanisms involved in the initiation of GX biosynthesis.

Materials and Methods

Gene expression analysis

For analysis of gene expression in different cell types, interfascicular fiber cells, xylem cells and pith cells from

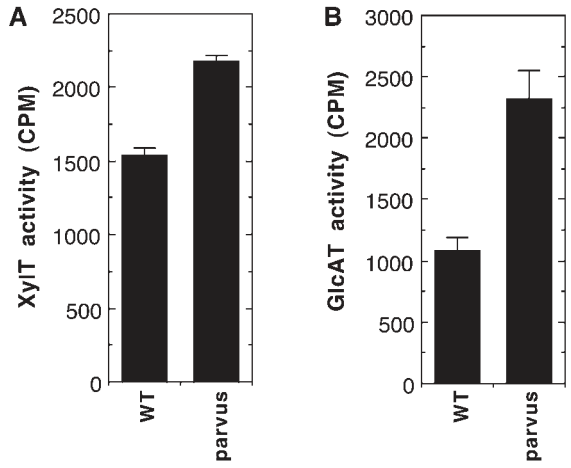

Fig. 9 The XylT and GlcAT activities in the stems of the wild type and *parvus* mutant. Microsomes isolated from the stems of the wild type and *parvus* mutant were incubated with Xyl_6 and UDP-[^{14}C]Xyl or UDP-[^{14}C]GlcA, and the XylT and GlcAT activities were detected by counting the radioactivity (CPM) of the reaction products. Error bars represent the SE of two separate assays. (A) XylT activity in the *parvus* mutant compared with the wild type. (B) GlcAT activity in the *parvus* mutant compared with the wild type.

inflorescence stems of 6-week-old *Arabidopsis* plants were isolated using the PALM microlaser system (PALM Microlaser Technologies, Bernried, Germany), and used for RNA isolation and amplification as described (Zhong et al. 2006). For analysis of gene expression in different organs, total RNA was isolated from leaves, roots, stems and flowers of 6-week-old *Arabidopsis* plants using a Qiagen RNA isolation kit (Valencia, CA, USA).

For quantitative PCR analysis, total RNA was treated with DNase I and used for first-strand cDNA synthesis. The first-strand cDNA was then used as template for real-time quantitative PCR analysis using gene-specific primers (5′-gtacacgtcacgcatcgaagag-3′ and 5′-agaatccaacgcgaacggcgtttg-3′) with the QuantiTect SYBR Green PCR Kit (Clontech, Mountain View, CA, USA). The relative mRNA levels were determined by normalizing the PCR threshold cycle number of each gene with that of the *EF1α* reference gene. The expression level of each gene in the wild-type control or in the sample with the lowest expression level was set to 1, and the data were the average of three replicates.

In situ localization of mRNAs

Wild-type *Arabidopsis* inflorescence stems were used for in situ mRNA localization as described (McAbee et al. 2005). Tissues were fixed in 2.5% formaldehyde and 0.5% glutaraldehyde, and then embedded in paraffin. Sections 10 μm thick were cut, mounted onto slides, and hybridized with digoxigenin-labeled *PARVUS* antisense RNA probe synthesized using the DIG RNA labeling mix (Roche, Mannheim, Germany). The *PARVUS* cDNA sequence used for RNA probe synthesis was PCR-amplified using gene-specific primers (5′-ccgacgcttcttccttacgag-3′ and 5′-ggtttaatcaaaccggcaaaaacc-3′) and this sequence shows no significant homology with other GTs. The hybridization and washing conditions used only allowed specific hybridization of the RNA probe to the *PARVUS* mRNA. The hybridization signals were detected with alkaline phosphatase-conjugated antibodies against digoxigenin and subsequent color development with alkaline phosphatase substrates.

Subcellular localization of fluorescent protein-tagged proteins

The co-localization of fluorescent protein-tagged PARVUS with the Golgi and ER markers was carried out in carrot protoplasts as described (Zhong et al. 2005a). The PARVUS cDNA was fused in-frame with the YFP cDNA and ligated between the cauliflower mosaic virus 35S promoter and the nopaline synthase terminator in a high copy vector. The fusion protein thus generated will have the YFP tag at the C-terminus. The PARVUS–YFP construct was co-transfected into carrot protoplasts together with CFP-tagged FRA8, a protein known to be localized in the Golgi (Zhong et al. 2005a), or with a CFP-tagged ER marker that was generated by fusing an *Arabidopsis* chitinase signal peptide to the N-terminus and an HDEL sequence to the C-terminus of CFP (Batoko et al. 2000). After a 20 h incubation, the transfected protoplasts were examined for yellow and cyan fluorescent signals using a Leica TCs SP2 spectral confocal microscope.

Immunolocalization of xylan

Basal stem internodes and roots of 10-week-old plants were fixed with 2% glutaraldehyde in phosphate-buffered saline (PBS), dehydrated through a gradient of ethanol, and then embedded in LR White Resin (Electron Microscopy Sciences, Fort Washington, PA, USA). Sections 1 μm thick were cut with a microtome and incubated with the LM10 monoclonal antibody, which recognizes glucuronoxylan (Plantprobes, Leeds, UK; McCartney et al. 2005) and then with fluorescein isothiocyanate-conjugated secondary antibodies. The fluorescence-labeled sections were observed using a Leica TCs SP2 spectral confocal microscope. Images from single optical sections were collected and processed with Adobe Photoshop.

Breaking force measurement

The main inflorescences of 10-week-old wild type *Arabidopsis* and *parvus* plants were divided into three equal segments, which were measured for their breaking force using a digital force/length tester (Model DHT4-50; Larson System, Minneapolis, MN, USA). The breaking force (g) was calculated as the force needed to break apart a stem segment (Zhong et al. 1997).

Histology

Basal stem internodes and roots of 10-week-old plants were fixed with 2% glutaraldehyde in PBS at 4°C overnight. After fixation, tissues were post-fixed in 1% (v/v) OsO_4, dehydrated through a gradient of ethanol, embedded in Spurr's resin (Electron Microscopy Sciences) and then subjected to sectioning with a microtome (Burk et al. 2006). Sections 1 μm thick were stained with toluidine blue for light microscopy. For transmission electron microscopy, 85 nm thick sections were stained with uranyl acetate and lead citrate, and visualized using a Zeiss EM 902A transmission electron microscope.

Cell wall isolation and extraction

Inflorescence stems of 10-week-old plants were collected for cell wall isolation. Stems were ground into a fine powder in liquid nitrogen with a motar and pestle, and homogenized sequentially in 70% ethanol and 100% acetone with a polytron. The resulting cell wall residues were dried in a vacuum oven at 60°C. The wall preparations were subsequently subjected to sequential extractions

with ammonium acetate (50 mM, 24 h), 1 N KOH containing 1% (w/v) $NaBH_4$ (24 h), and 4 N KOH containing 1% (w/v) $NaBH_4$ (24 h) according to Zhong et al. (2005b). The 1 and 4 N KOH-soluble extracts were passed through a glass fiber filter, neutralized to pH 6.0 with glacial acetic acid, dialyzed in a dialysis tubing (3,500 M_r cut-off; Fisher Scientific, Pittsburgh, PA, USA) against deionized water, and lyophilized.

Cell wall composition analysis

Cell wall sugars (as alditol acetates) were determined following the procedure described by Hoebler et al. (1989). Briefly, cell walls were incubated with 70% sulfuric acid at 37°C for 60 min followed by addition of inositol as the internal standard and dilution with water to 2 N sulfuric acid. After heating for 120 min at 100°C, the solution was cooled and treated with 25% ammonium solution. After reduction with sodium borohydride in dimethylsulfoxide, the solution was heated for 90 min at 40°C, followed by sequential treatment with glacial acetic acid, acetic anhydride, 1-methylimidazole, dichloromethane and water. The organic layer containing the alditol acetates of the hydrolyzed cell wall sugars was washed three times with water, and sugars were analyzed on an Agilent 6890N gas–liquid chromatograph (Wilmington, DE, USA) equipped with a 30 m × 0.25 mm (i.d.) silica capillary column DB 225 (Alltech Assoc., Deerfield, IL, USA).

Generation of xylooligosaccharides with β-endoxylanase

The 1 and 4 N KOH-solubilized wall preparations were digested with β-xylanase M6 (Megazyme, Wicklow, Ireland) for generation of xylooligosaccharides as described (Zhong et al. 2005b). The released xylooligosaccharides were desalted and separated by size exclusion chromatography on a Sephadex G-25 column (100 × 2.5 mm). Fractions containing the oligosaccharides were determined by the phenol–sulfuric assay (DuBois et al. 1956), pooled and lyophilized.

Matrix-assisted laser-desorption ionization time-of-flight mass spectrometry (MALDI-TOF MS)

The acidic xylooligosaccharides released from β-xylanase digestion were analyzed using a MALDI-TOF mass spectrometer operated in the positive-ion mode with an accelerating voltage of 30 kV, an extractor voltage of 9 kV and a source pressure of approximately 8×10^{-7} torr. The aqueous sample was mixed (1 : 1, v/v) with the MALDI matrix (0.2 M 2,5-dihydroxybenzoic acid and 0.06 M 1-hydroxyisoquinoline in 50% acetonitrile) and dried on the stainless steel target plate. Spectra are the average of 100 laser shots.

^{1}H-NMR spectroscopy

NMR spectra of the acidic xylooligosaccharides from β-xylanase digestion were recorded at 298 K with an NMR spectrometer. Chemical shifts were measured relative to internal acetone at δ 2.225. The ^{1}H-NMR assignments were done by comparison with the NMR spectra data for *Arabidopsis* acidic xylooligosaccharides (Zhong et al. 2005b, Pena et al., 2007) and further confirmed by two-dimensional gCOSY, HSQC, HMBC and TOCSY spectra.

Assay of GlcAT and XylT activities

Microsomes were isolated and the GlcAT and XylT activities were determined following the procedures of Kuroyama and Tsumuraya (2001). For assay of GlcAT activity, 100 µg of microsomes were incubated with the reaction mixture (a total volume of 30 µl) containing 50 mM HEPES-KOH, pH 6.8, 5 mM $MnCl_2$, 1 mM dithiothreitol (DTT), 0.5% Triton X-100, 0.2 µg µl^{-1} Xyl_6 (Megazyme) and UDP-[^{14}C]GlcA (0.1 µCi; American Radiolabeled Chemical, St Louis, MO, USA). For assay of XylT activity, 100 µg of microsomes were incubated with the reaction mixture (a total volume of 30 µl) containing 50 mM HEPES-KOH, pH 6.8, 5 mM $MnCl_2$, 1 mM DTT, 0.5% Triton X-100, 0.1 mM cold UDP-Xyl (CarboSource Service, Athens, GA, USA; supported in part by NSF-RCN grant #0090281), 0.2 µg µl^{-1} Xyl_6 and UDP-[^{14}C]Xyl (0.1 µCi; American Radiolabeled Chemical). After incubation at 21°C for 20 min, the reactions were stopped by addition of the termination solution (0.3 M acetic acid containing 20 mM EGTA). The radiolabeled xylooligosaccharides were separated from UDP-[^{14}C]Xyl or UDP-[^{14}C]GlcA by paper chromatography according to Ishikawa et al. (2000), and the incorporation of radiolabeled Xyl or GlcA onto xylooligosaccharides was determined with a PerkinElmer scintillation counter (Waltham, MA, USA).

Funding

The US Department of Energy-Bioscience Division (Grant # DE-FG02-03ER15415); the Korea Science and Engineering Foundation (Grant # KRF-2005-215-F00002) to C.H.L.

Acknowledgments

We thank N.S. Hill for his help on the lyophilization of samples, M. A. O'Neill for his suggestions on GX analysis, and the editor and the reviewers for their comments and suggestions.

References

Andersson, S.-I., Samuelson, O., Ishihara, M. and Shimizu, K. (1983) Structure of the reducing end-groups in spruce xylan. *Carbohydr. Res.* 111: 283–288.

Aspeborg, H., Schrader, J., Coutinho, P.M., Stam, M., Kallas, A., et al. (2005) Carbohydrate-active enzymes involved in the secondary cell wall biogenesis in hybrid aspen. *Plant Physiol.* 137: 983–997.

Batoko, H., Zheng, H.-Q., Hawes, C. and Moore, I. (2000) A Rab1 GTPase is required for transport between the endoplasmic reticulum and Golgi apparatus and for normal Golgi movement in plants. *Plant Cell* 12: 2201–2217.

Bauer, S., Vasu, P., Persson, S., Mort, A.J. and Somerville, C.R. (2006) Development and application of a suite of polysaccharide-degrading enzymes for analyzing plant cell walls. *Proc. Natl Acad. Sci. USA* 103: 11417–11422.

Baydoun, E.A.-H., Usta, J.A.-R., Waldron, K.W. and Brett, C.T. (1989) A methyltransferase involved in the biosynthesis of 4-*O*-methylglucuronoxylan in etiolated pea epicotyls. *J. Plant Physiol.* 135: 81–85.

Baydoun, E.A.-H., Waldron, K.W. and Brett, C.T. (1983) The interaction of xylosyltransferase and glucuronyltransferase involved in glucuronoxylan synthesis in pea (*Pisum sativum*) epicotyls. *Biochem. J.* 257: 853–858.

Bouton, S., Leboeuf, E., Mouille, G., Leydecker, M.-T., Talbotec, J., Grainier, F., Lahaye, M., Höfte, H. and Truong, H.-N. (2002) *QUASIMODO1* encodes a putative membrane-bound glycosyltransferase required for normal pectin synthesis and cell adhesion in *Arabidopsis*. *Plant Cell* 14: 2577–2590.

Brown, D.M., Zeef, L.A.H., Ellis, J., Goodacreb, R. and Turner, S.R. (2005) Identification of novel genes in *Arabidopsis* involved in secondary

cell wall formation using expression profiling and reverse genetics. *Plant Cell* 17: 2281–2295.

Burk, D.H., Zhong, R., Morrison, W.H.III and Ye, Z.-H. (2006) Disruption of cortical microtubules by overexpression of green fluorescent protein-tagged α-tubulin 6 causes a marked reduction in cell wall synthesis. *J. Integr. Plant Biol.* 48: 85–98.

Coutinho, P.M., Deleury, E., Davies, G.J. and Henrissat, B. (2003) An evolving hierarchical family classification for glycosyltransferases. *J. Mol. Biol.* 328: 307–317.

Crosthwaite, S.K., MacDonald, F.M., Baydoun, E.A.-H. and Brett, C.T. (1994) Properties of a protein-linked glucuronxylan formed in the plant Golgi apparatus. *J. Exp. Bot.* 45: 471–475.

Dalessandro, G. and Northcote, D.H. (1981) Increase of xylan synthetase activity during xylem differentiation of the vascular cambium of sycamore and poplar trees. *Planta* 151: 61–67.

DuBois, M., Gilles, K.A., Hamilton, J.K., Rebers, P.A. and Smith, F. (1956) Colorimtric method for determination of sugars and related substances. *Anal. Chem.* 28: 350–356.

Ebringerová, A. and Heinze, T. (2000) Xylan and xylan derivatives—biopolymers with valuable properties, 1. Naturally occurring xylans structures, isolation procedures and properties. *Macromol. Rapid Commun.* 21: 542–556.

Gregory, A.C.E., Smith, C., Kerry, M.E., Wheatley, E.R. and Bolwell, G.P. (2002) Comparative subcellular immunolocation of polypeptides associated with xylan and callose synthases in French bean (*Phaseolus vulgaris*) during secondary wall formation. *Phytochemistry* 59: 249–259.

Hoebler, C., Barry, J.L., David, A. and Delort-Laval, J. (1989) Rapid acid-hydrolysis of plant cell wall polysaccharides and simplified quantitative determination of their neutral monosaccharides by gas–liquid chromatography. *J. Agric. Food Chem.* 37: 360–367.

Ishikawa, M., Kuroyama, H., Takeuchi, Y. and Tsumuraya, Y. (2000) Characterization of pectin methyltransferase from soybean hypocotyls. *Planta* 210: 782–791.

Johansson, M.H. and Samuelson, O. (1977) Reducing end groups in birch xylan and their alkaline degradation. *Wood Sci. Technol.* 11: 251–263.

Kuroyama, H. and Tsumuraya, Y. (2001) A xylosyltransferase that synthesizes β-(1 → 4)-xylans in wheat (*Triticum aestivum* L.) seedlings. *Planta* 213: 231–240.

Lao, N.T., Long, D., Kiang, S., Coupland, G., Shoue, D.A., Carpita, N.C. and Kavanagh, T.A. (2003) Mutation of a family 8 glycosyltransferase gene alters cell wall carbohydrate composition and causes a humidity-sensitive semi-sterile dwarf phenotype in *Arabidopsis*. *Plant Mol. Biol.* 53: 687–701.

Lee, C., O'Neill, M.A., Tsumuraya, Y., Darvill, A.G. and Ye, Z.-H. (2007) The *irregular xylem9* mutant is deficient in xylan xylosyltransferase activity. *Plant Cell Physiol.* 48: 1624–1634.

Lerouxel, O., Cavalier, D.M., Liepman, A.H. and Keegstra, K. (2006) Biosynthesis of plant cell wall polysaccharides—a complex process. *Curr. Opin. Plant Biol.* 9: 621–630.

McAbee, J.M., Kuzoff, R.K. and Gasser, C.S. (2005) Mechanisms of derived unitegmy among impatiens species. *Plant Cell* 17: 1674–1684.

McCartney, L., Marcus, S.E. and Knox, J.P. (2005) Monoclonal antibodies to plant cell wall xylans and arabinoxylans. *J. Histochem. Cytochem.* 53: 543–546.

Pena, M.J., Zhong, R., Zhou, G.-K., Richardson, E.A., O'Neill, M.A., Darvill, A.G., York, W.S. and Ye, Z.-H. (2007) *Arabidopsis irregular xylem8* and *irregular xylem9*: implications for the complexity of glucuronoxylan biosynthesis. *Plant Cell* 19: 549–563.

Persson, S., Caffall, K.H., Freshour, G., Hilley, M.T., Bauer, S., Poindexter, P., Hahn, M.G., Mohnen, D. and Somerville, C. (2007) The *Arabidopsis irregular xylem8* mutant is deficient in glucuronoxylan and homogalacturonan, which are essential for secondary cell wall integrity. *Plant Cell* 19: 237–255.

Persson, S., Wei, H., Miline, J., Page, G.P. and Somerville, C.R. (2005) Identification of genes required for cellulose synthesis by repression analysis of public microarray data sets. *Proc. Natl Acad. Sci. USA* 102: 8633–8638.

Porchia, A.C. and Scheller, H.V. (2000) Arabinoxylan biosynthesis: identification and partial characterization of β-1,4-xylosyltransferase from wheat. *Physiol. Plant* 110: 350–356.

Porchia, A.C., Sorensen, S.O. and Scheller, H.V. (2002) Arabinoxylan biosynthesis in wheat. Characterization of arabinosyltransferase activity in Golgi membranes. *Plant Physiol.* 130: 432–441.

Prydz, K. and Dalen, K.T. (2000) Synthesis and sorting of proteoglycans. *J. Cell Sci.* 11: 193–205.

Shao, M., Zheng, H., Hu, Y., Liu, D., Jang, J.-C., Ma, H. and Huang, H. (2004) The *GAOLAOZHUANGREN1* gene encodes a putative glycosyltransferase that is critical for normal development and carbohydrate metabolism. *Plant Cell Physiol.* 45: 1453–1460.

Shimizu, K., Ishihara, M. and Ishihara, T. (1976) Hemicellulases of brown rotting fungus, *Tyromyces palustris*. II. The oligosaccharides from the hydrolysate of a hardwood xylan by the intracellular xylanase. *Mokuzai Gaikkashi.* 22: 618–625.

Sterling, J.D., Atmodjo, M.A., Inwood, S.E., Kumar Kolli, V.S., Quigley, H.F., Hahn, M.G. and Mohnen, D. (2006) Functional identification of an *Arabidopsis* pectin biosynthetic homogalacturonan galacturonosyltransferase. *Proc. Natl Acad. Sci. USA* 103: 5236–5241.

Suzuki, K., Ingold, E., Sugiyama, M. and Komamine, A. (1991) Xylan synthase activity in isolated mesophyll cells of *Zinnia elegans* during differentiation to tracheary elements. *Plant Cell Physiol.* 32: 303–306.

Urahara, T., Tsuchiya, K., Kotake, T., Tohno-oka, T., Komae, K., Kawada, N. and Tsumuraya, Y. (2004) A β-(1 → 4)-xylosyltransferase involved in the synthesis of arabinoxylans in developing barley endosperms. *Physiol. Plant* 122: 169–180.

Willats, W.G.T., McCartney, L., Mackie, W. and Knox, J.P. (2001) Pectin: cell biology and prospects for functional analysis. *Plant Mol. Biol.* 47: 9–27.

Ye, Z.-H., Freshour, G., Hahn, M.G., Burk, D.H. and Zhong, R. (2002) Vascular development in *Arabidopsis*. *Int. Rev. Cytol* 220: 225–256.

Zhong, R., Burk, D.H., Nairn, C.J., Wood-Jones, A., Morrison, W.H., , III and Ye, Z.-H. (2005a) Mutation of SAC1, an *Arabidopsis* SAC domain phosphoinositide phosphatase, causes alterations in cell morphogenesis, cell wall synthesis, and actin organization. *Plant Cell* 17: 1449–1466.

Zhong, R., Burk, D.H. and Ye, Z.-H. (2001) Fibers. A model for studying cell differentiation, cell elongation, and cell wall biosynthesis. *Plant Physiol.* 126: 477–479.

Zhong, R., Demura, T. and Ye, Z.-H. (2006) SND1, a NAC domain transcription factor, is a key regulator of secondary wall synthesis in fibers of *Arabidopsis*. *Plant Cell* 18: 3158–3170.

Zhong, R., Pena, M.J., Zhou, G.-K., Nairn, C.J., Wood-Jones, A., Richardson, E.A., Morrison, W.H., Darvill, A.G., York, W.S. and Ye, Z.-H. (2005b) *Arabidopsis Fragile Fiber8*, which encodes a putative glucuronyltransferase, is essential for normal secondary wall synthesis. *Plant Cell* 17: 3390–3408.

Zhong, R., Richardson, E.A. and Ye, Z.-H. (2007a) The MYB46 transcription factor is a direct target of SND1 and regulates secondary wall biosynthesis in *Arabidopsis*. *Plant Cell* 19: 2776–2792.

Zhong, R., Richardson, E.A. and Ye, Z.-H. (2007b) Two NAC domain transcription factors, SND1 and NST1, function redundantly in regulation of secondary wall synthesis in fibers of *Arabidopsis*. *Planta* 225: 1603–1611.

Zhong, R., Taylor, J.J. and Ye, Z.-H. (1997) Disruption of interfascicular fiber differentiation in an *Arabidopsis* mutant. *Plant Cell* 9: 2159–2170.

Zhou, G.K., Zhong, R., Richardson, E.A., Himmelsbach, D.S., McPhail, B.T. and Ye, Z.-H. (2007) Molecular characterization of PoGT8D and PoGT43B, two secondary wall-associated glycosyltransferases in poplar. *Plant Cell Physiol.* 48: 689–699.

Zhou, G.K., Zhong, R., Richardson, E.A., Morrison, W.H., 3rd, Nairn, C.J., Wood-Jones, A. and Ye, Z.-H. (2006) The poplar glycosyltransferase GT47C is functionally conserved with *Arabidopsis Fragile Fiber8*. *Plant Cell Physiol.* 47: 1229–1240.

(Received October 24, 2007; Accepted November 5, 2007)